Tagging of plant potyvirus replication and movement by insertion of β-glucuronidase into the viral polyprotein

(cell-to-cell movement/plant expression vector/symptomatology/tobacco etch virus)

VALERIAN V. DOLJA, HELEN J. MCBRIDE, AND JAMES C. CARRINGTON

Department of Biology, Texas A&M University, College Station, TX 77843

ABSTRACT Infectious RNA transcripts were generated from full-length cDNA clones of the tobacco etch potyvirus genome containing an insertion of the bacterial β-glucuronidase (GUS) gene between the polyprotein-coding sequences for the N-terminal 35-kDa proteinase and the helper component–proteinase. The recombinant virus was able to spread systemically in plants and accumulated to a level comparable with wild-type tobacco etch potyvirus. Proteolytic processing mediated by the 35-kDa proteinase and helper component–proteinase resulted in production of an enzymatically active GUS–helper component-proteinase fusion protein. A virus passage line that retained the GUS insert after numerous plant-to-plant transfers, as well as a line that sustained a deletion of the GUS sequence, was recovered. Use of an *in situ* histochemical GUS assay in time-course experiments allowed the visualization of virus activity in single, mechanically inoculated leaf epidermal cells, in neighboring epidermal and mesophyll cells, in phloem-associated cells after long-distance transport, and in cells surrounding vascular tissues of organs above and below the site of inoculation. This system represents a powerful tool to study plant virus replication, short- and long-distance virus movement, and virus–host interactions. Additionally, we show that potyviruses may serve as highly efficient, autonomously replicating vectors for the expression of foreign genes in plants.

Tobacco etch virus (TEV), a well-characterized potyvirus, contains a positive-strand RNA genome of 9.5 kilobases (kb) coding for a single, large polyprotein that is processed by three virus-specific proteinases (Fig. 1 and refs. 1 and 2). The nuclear inclusion protein "a" proteinase is involved in the maturation of several replication-associated proteins and capsid protein (3). The helper component–proteinase (HC-Pro) and 35-kDa proteinase both catalyze cleavage only at their respective C termini (4, 5). The proteolytic domain in each of these proteins is located near the C terminus. For HC-Pro, the N-terminal domain is required for virus transmission by aphids (6). The 35-kDa proteinase and HC-Pro derive from the N-terminal region of the TEV polyprotein (Fig. 1). Unlike the events associated with proteolytic processing, relatively little is known regarding the requirements for potyviral RNA replication and virus transport.

The production of full-length, infectious RNA transcripts from cloned cDNAs representing plant positive-strand RNA virus genomes has permitted the analysis of many viral functions, including RNA replication and cell-to-cell movement (e.g., refs. 7–10). In addition, infectious transcripts from cDNA have allowed the construction of RNA-based vectors for expression of foreign genes in plants (11–13). Although a high level of replication is an attractive feature of a putative RNA virus vector, the use of RNA vectors has

been limited due to instability of inserted foreign sequences and disruption of systemic virus spread after replacement of virus genes involved in movement.

The generation of infectious clones of the TEV genome carrying a copy of the reporter gene β-glucuronidase (GUS) is described in this paper. Virus derived from this clone was used as a highly sensitive probe to analyze cell-to-cell and long-distance movement of TEV in plants. This system should permit exploration of additional aspects of virus function and virus–host interactions in intact plants. It was also demonstrated that TEV and potyviruses, in general, may serve as efficient plant expression vectors.

MATERIALS AND METHODS

Plasmid Constructions. A nearly full-length DNA copy of TEV RNA was synthesized with reverse transcriptase (SuperScript from GIBCO-BRL) and a primer complementary to 23 nucleotides (nt) preceding the 3′-terminal poly(A) tail of the virus genome. Double-stranded DNA was generated using *Escherichia coli* DNA polymerase I and RNase H, digested with *Bst*EII, and inserted into *Bst*EII-digested pTL7SN.3-0027, which contains sequences representing the 5′ and 3′ ends of the TEV genome as described (14). A unique *Bgl* II site was engineered immediately after the 25-nt 3′ poly(A) tail by site-directed mutagenesis (15). A longer poly(A) tail (70–75 nt) was incorporated from pBB5995 (from W. G. Dougherty, Oregon State University), resulting in pTEV7D (Fig. 1). Plasmids were propagated in *E. coli* strain HB101.

Site-directed mutagenesis (15) was used to introduce *Nco* I sites flanking the 5′ and 3′ terminal coding sequences of the GUS gene in pTL7SN.3-GUS (16). The GUS coding region was excised with *Nco* I and inserted into the *Nco* I site that was introduced near the beginning of the HC-Pro coding sequence in pTL7SN.3-0627 (5). The GUS gene and adjacent TEV coding sequences from this plasmid were incorporated into pTEV7D, resulting in pTEV7D-GUS.HC (Fig. 1). The GUS gene was also inserted into the *Nco* I site that had been introduced previously at the beginning of the 35-kDa protein coding region in pTL7SN.3-0027 (14). The GUS and adjacent TEV sequences from the resulting plasmid were introduced into pTEV7D, yielding pTEV7D-GUS.P1 (Fig. 1).

In Vitro **Transcription and Inoculation of Plants.** Transcripts that were capped with 7-methylguanosine(5′)triphospho (5′)guanosine were synthesized using bacteriophage SP6 RNA polymerase and cesium chloride-purified, *Bgl* II-linearized plasmid DNA as described (16). The 5′ ends of transcripts from pTEV7D and related plasmids contained two additional nonviral nucleotides. Transcription mixtures were diluted with equal volumes (vol) of 10 mM sodium phosphate

Abbreviations: GUS, β-glucuronidase; TEV, tobacco etch virus; HC-Pro, helper component–proteinase; nt, nucleotide(s); p.i., post-inoculation; X-gluc, 5-bromo-4-chloro-3-indolyl β-D-glucuronic acid, cyclohexylammonium salt.

Genetics: Dolja *et al.*
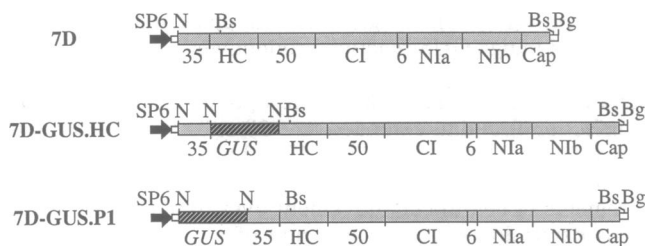
Proc. Natl. Acad. Sci. USA 89 (1992)   10209

FIG. 1. Diagrams of portions of plasmids containing cDNA representing the complete TEV genome and inserted GUS gene. The noncoding (open boxes) and coding (stippled shading) regions of the TEV genome, the GUS gene (hatched shading), and SP6 RNA polymerase promoter (black arrow) are shown. Vertical lines below maps indicate sequences coding for proteolytic processing sites, whereas selected restriction sites are indicated above maps. The suffixes of plasmid names given in text are indicated at left. N, *Nco* I; Bs, *Bst*EII; Bg, *Bgl* II; 35, 35-kDa proteinase; HC, HC-Pro; 50, 50-kDa TEV protein; CI, cylindrical inclusion protein; 6, 6-kDa TEV protein; NIa, nuclear inclusion protein a; NIb, nuclear inclusion protein b; Cap, capsid protein; 7D, pTEV7D.

buffer, pH 7.4, and applied manually onto young tobacco plants (10 μl per leaf, two leaves per plant) with the aid of carborundum. In passage experiments, infected leaves were ground in 10 vol of 10 mM sodium phosphate buffer containing carborundum and applied manually to leaves of healthy plants with a cotton swab.

GUS Assays and Immunoblot Analysis. Fluorometric assays for GUS activity and measurements of protein concentration were conducted as described (16). *In situ* GUS assays were done by using a colorimetric substrate according to Restrepo *et al.* (17). Tobacco leaves were vacuum infiltrated with the substrate 5-bromo-4-chloro-3-indolyl β-D-glucuronic acid, cyclohexylammonium salt (X-gluc) (1.2 mM) in 0.5 mM potassium ferricyanide/0.5 mM potassium ferrocyanide/10 mM EDTA. Manual cross-sections of leaf petioles, stems, and roots were placed directly into the substrate solution and photographed under bright-field optics by using a Zeiss photomicroscope. Total SDS-soluble proteins were extracted from leaf tissue by grinding in 7 vol of protein dissociation buffer (0.625 M Tris·HCl, pH 6.8/2% SDS/10% 2-mercaptoethanol/10% (vol/vol) glycerol) and subjected to immunoblot analysis with anti-HC-Pro (14), anti-capsid (17), or anti-GUS (from Tom McKnight, Texas A & M University) sera by described procedures (14).

RESULTS

Insertion and Expression of GUS Gene in TEV Genome. Approximately 27% (15 of 56) of tobacco plants inoculated with capped RNA transcripts derived from pTEV7D became infected. Using the PCR, RNA isolated from progeny virions was shown to contain the sequence corresponding to the *Nco* I site engineered at the start codon for TEV polyprotein in pTEV7D (data not shown), demonstrating the transcript-derived origin of infection. Twenty-five percent (16 of 64) and 0% (0 of 16) of plants inoculated with pTEV7D-GUS.HC and pTEV7D-GUS.P1 transcripts, respectively, became infected. Due to the absence of infectivity, pTEV7D-GUS.P1 was not used further. Virion RNA from pTEV7D-GUS.HC transcript-inoculated plants exhibited decreased electrophoretic mobility compared with RNA from wild-type TEV, suggesting that the GUS gene was retained in progeny virus. Plants infected by the modified virus, which will be referred to as TEV–GUS, lacked the vein clearing and etching typical of plants infected by wild-type TEV.

The GUS gene in pTEV7D-GUS.HC was inserted adjacent to the coding sequence for the 35-kDa proteinase autoproteolytic cleavage site at Tyr-304/Ser-305 (18) between the

35-kDa proteinase and HC-Pro. Insertion of GUS into the polyprotein at this position has been shown not to interfere with the 35-kDa proteinase processing activity (5). Proteolysis by 35-kDa proteinase and HC-Pro at their respective C termini was predicted to yield a GUS–HC-Pro fusion protein of ≈119 kDa. Immunoblot analysis of protein extracts from two pTEV7D-GUS.HC transcript-inoculated plants revealed accumulation of a ≈119-kDa product that reacted with both anti-HC-Pro and anti-GUS sera (Fig. 2, lanes 8, 9, 12, and 13). Plants inoculated with transcripts from pTEV7D, on the other hand, contained HC-Pro of normal size (52 kDa) that reacted only with anti-HC-Pro serum (lanes 10 and 14). Immunoblot analysis using anti-capsid serum indicated that the levels of capsid protein in plants inoculated with pTEV7D-GUS.HC and pTEV7D transcripts were similar (lanes 4–6). By comparing the level of immunoreactive protein in preparations of known protein concentration against a standard series, capsid protein was shown to account for ≈1% of total protein in extracts from plants inoculated with transcripts from either plasmid (lanes 1–6).

The stability of the GUS insert within the TEV–GUS genome was assayed by immunoblot analysis in plant-to-plant passage experiments using virus originally recovered from two plants (plant 3 and 7) infected with RNA transcripts. All passages were performed 4–6 days postinoculation (p.i.), except passage II (16 days p.i.). The 119-kDa GUS–HC-Pro protein was intact after seven passages of virus from plant 3 (Fig. 3, lanes 2, 4, 6, 8, and 11), suggesting stable retention of the GUS sequence. By use of a fluorometric assay, GUS activity levels were determined to be comparable in plants from each passage, as well as from an additional seven passages (data not shown). In contrast, TEV–GUS from plant 7 sustained a deletion in the GUS–HC-Pro coding region that was evident during passage IV, resulting in appearance of an anti-HC-Pro reactive protein that was ≈7 kDa smaller than intact HC-Pro (lanes 7, 9, and 10). This form was also detected in the remaining three passages (lanes 1, 3, and 5). The disappearance of the GUS–HC-Pro protein correlated with a loss of GUS activity, as well as a reversion to a mosaic- and etch-inducing phenotype, in plants from passages V–VII (data not shown).
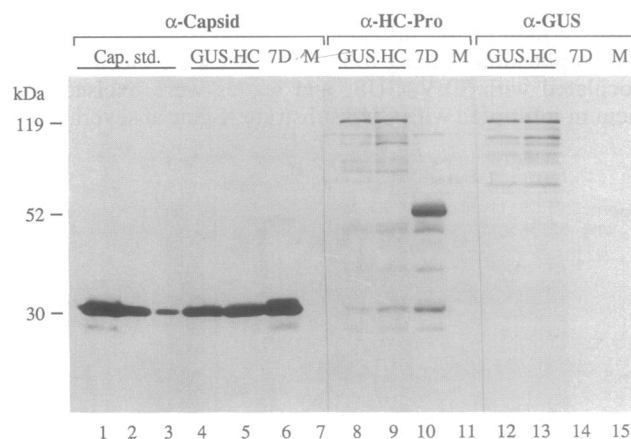

FIG. 2. Immunoblot analysis of extracts from RNA transcript-inoculated tobacco plants. Extracts from pTEV7D (7D; lanes 6, 10, and 14), two pTEV7D-GUS.HC (lanes 4, 5, 8, 9, 12, 13)-infected plants, and a mock-inoculated plant (M; lanes 7, 11, and 15) were analyzed by using anti-capsid protein, anti-HC-Pro, or anti-GUS serum. Lanes 4–15 each contained ≈50 μg of SDS-soluble protein. A capsid protein concentration series (capsid standard; Cap. std.) consisting of 1.0 μg, 0.1 μg, and 0.01 μg (lanes 1–3, respectively) was also analyzed. The molecular masses (in kDa) of capsid protein (30 kDa), HC-Pro (52 kDa), and the GUS–HC-Pro fusion protein (119 kDa) are located at left. The minor immunoreactive bands in lanes 8–10, 12, and 13 represent degradation products.
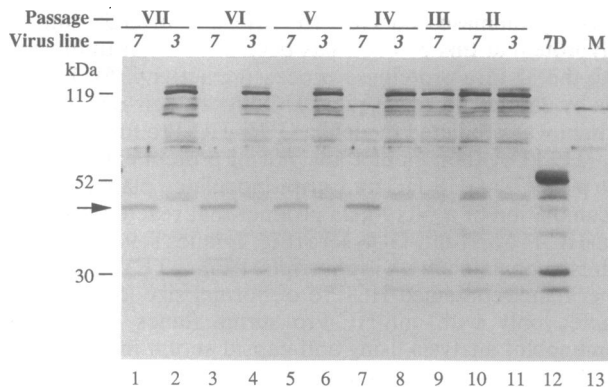
FIG. 3. Immunoblot analysis of extracts from tobacco plants infected by serially passaged TEV–GUS. Samples were prepared from plants representing two independent virus lineages that started from plants 3 and 7 infected with pTEV7D-GUS.HC RNA transcripts and were analyzed using anti-HC-Pro serum. Extracts from TEV–GUS passages II–VII (lanes 1–11), pTEV7D transcript-inoculated (7D; lane 12), and mock-inoculated (M; lane 13) plants are shown. For TEV–GUS passage I, see Fig. 2, lanes 8 and 9. The arrow shows the HC-Pro-related product encoded by TEV–GUS from passage line 7. See Fig. 2 legend for additional details.

The stability of TEV–GUS as a function of time after inoculation was tested by using virus from passage line 3. Upper systemic leaves from passage V and VI plants were screened for GUS–HC-Pro fusion protein by immunoblot analysis and for GUS activity by using a fluorometric assay at intervals after inoculation. Deletions that resulted in truncated fusion proteins were detected 20 and 25 days p.i. in passage VI and V plants, respectively (Fig. 4A, lanes 2 and 5, respectively). Additional deletion variants encoding HC-Pro-related proteins smaller than wild-type HC-Pro were evident after an additional 5 days in each plant (lanes 1, 4, and 7). The appearance of deleted forms correlated with decreased amounts of both the intact 119-kDa fusion protein (compare lanes 1 and 2 with lane 3, and lanes 4 and 5 with lane 6) and GUS activity (Fig. 4B).

Visualization of Virus Infection and Movement. The synthesis of a GUS–HC-Pro fusion protein provides a highly sensitive marker for individual cells and tissues supporting virus replication. Young tobacco plants were mechanically inoculated with TEV–GUS, and leaves were excised and vacuum-infiltrated with GUS substrate X-gluc at several time
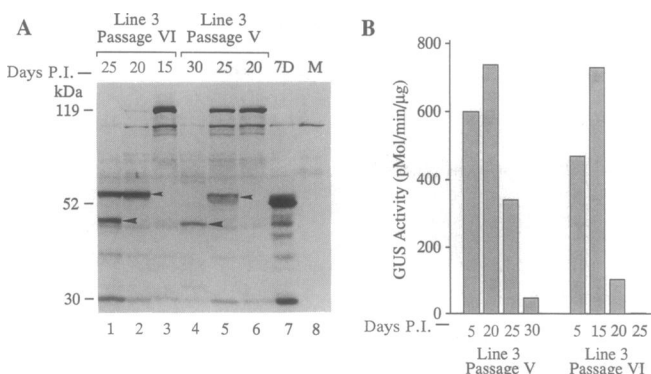

FIG. 4. Analysis of GUS–HC-Pro fusion protein and GUS activity in aging plants infected by TEV–GUS. (A) Extracts were prepared at the times p.i. indicated from upper systemic leaves of passage V and VI plants infected by TEV–GUS line 3 and were subjected to immunoblot analysis with anti-HC-Pro serum (lanes 1–6). Extracts were also analyzed from pTEV7D (7D; lane 7) and mock-inoculated (M; lane 8) plants. See Fig. 2 legend for additional details. (B) GUS activities as determined by fluorometric assay with extracts analyzed in A.

points p.i. (Fig. 5). Single infected epidermal cells that contained indigo GUS reaction product were identified 12 hr p.i. on primary inoculated leaves (B). By 24 hr p.i., movement to adjacent epidermal and mesophyll cells had resulted in infection foci that extended to ≈10 cells in diameter and that were visible by eye (C and D). These foci continued to expand and eventually fused by 96 hr p.i. (E and F). Measurements of cell-to-cell movement over time indicated that focus expansion occurred at a rate of ≈one cell per 2 hr. Activity of TEV–GUS was detected around segments of vascular tissue in systemically (noninoculated) infected leaves by 60 hr p.i. (H). After 72 hr p.i., virus movement was evident along major and minor veins and into leaf mesophyll cells adjacent to vascular tissue (I and K). Spread of virus through mesophyll tissue between veins proceeded at a rate comparable to that measured on inoculated leaves (K and L).

To determine which cells or cell types were infected first during systemic spread, cross-sections from stems, roots, and leaf petioles above the site of inoculation were incubated in X-gluc and visualized by light microscopy. No TEV–GUS activity was detected at 24 and 48 hr p.i. in any of the organs (Fig. 6, A, B, E, F, I, and J). By 72 hr p.i., however, clusters of phloem-associated cells in each of the three organs exhibited activity (C, G, and K). Nonphloem-associated cell types, such as xylem parenchyma and cortex, were free of detectable TEV–GUS. Ingress into these cell types was evident after 96 hr p.i. (D, H, and L). Strikingly, tissues of lateral roots contained especially high levels of activity (L).

DISCUSSION

We have used an infectious cDNA clone to introduce a marker gene into the TEV genome, and have demonstrated that virus replication and movement can be monitored easily by using a simple histochemical assay *in situ*. The GUS enzyme was incorporated into the TEV polyprotein and was proteolytically excised as a fusion product with a nonstructural protein, HC-Pro. This "tagged" virus was generated without the removal of any TEV sequences, and its reproduction and movement were not affected in any significant way. The most obvious difference between TEV and TEV–GUS infection, however, was the attenuated symptom phenotype of the latter virus.

The TEV–GUS from transcript-inoculated plant 3 was extremely stable upon rapid serial passage, although prolonged incubation of infected plants gave rise to deleted forms. It is possible that the sizable population of virus within older infected plants may provide a sufficiently large pool from which deletion variants with replicative or transport advantages can arise. In the rapid serial passage lines, the pool size may be limited due to the relatively few numbers of virus particles entering the inoculated plants and the short incubation period. Alternatively, the fidelity of viral RNA replication may be decreased in aging plants, thereby increasing the chances of deletion events after extended incubation. A long incubation period (16 days) of the passage II plants may have resulted in the deletion that appeared in plant 7-derived TEV–GUS, although this truncated variant would have had to remain a minor component of the virus pool until passage IV.

The GUS histochemical assay was used to investigate the time course of TEV–GUS infection in inoculated and systemic tissue. Compared with cytopathological and immunocytochemical methods used (19), the detection of GUS activity may be the most sensitive and simple way to monitor the timing of cell-to-cell movement. This activity should appear during the earliest stages (RNA replication and translation) of infection of a cell and should not diffuse freely to adjacent cells due to the low exclusion limit of plasmodesmata (20). Movement of virus out of initially infected epider-
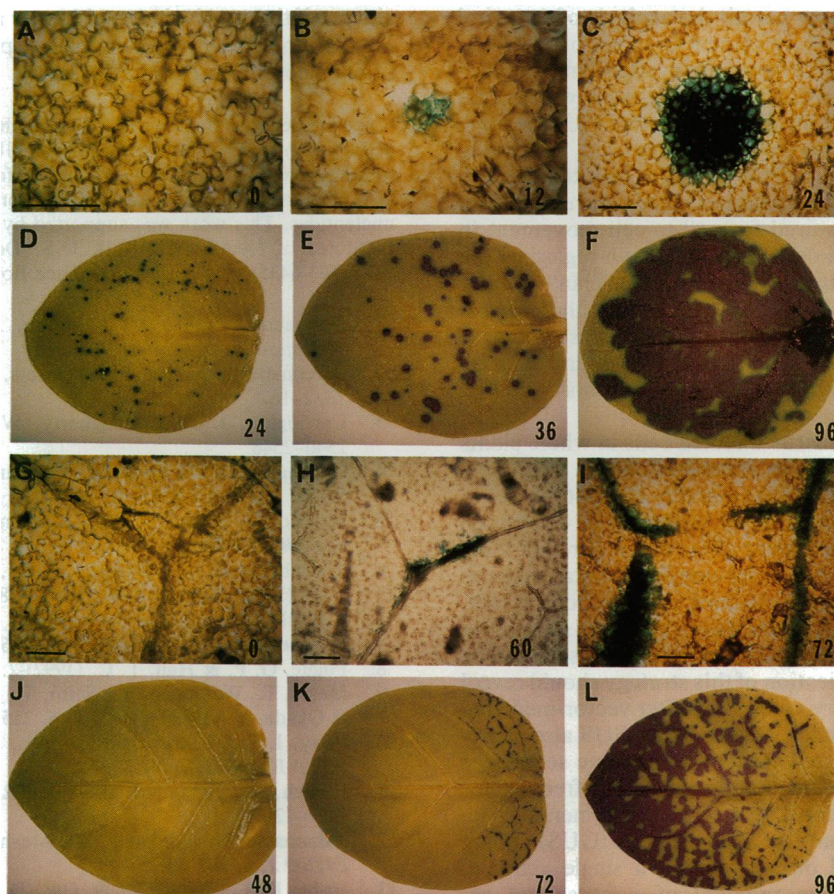
Genetics: Dolja *et al.*

Proc. Natl. Acad. Sci. USA 89 (1992)   10211

Fig. 5.   *In situ* localization of GUS activity in plants infected by TEV–GUS. Plants were inoculated with TEV–GUS at 100 μg/ml. Whole leaves were vacuum-infiltrated with the histochemical GUS substrate X-gluc at the times p.i. (hr) indicated at bottom right. (*A–F*) Microscopic (*A–C*) and macroscopic (*D–F*) visualization of GUS activity in primary inoculated leaves. Note that *B* contains a single GUS-positive epidermal cell. (*G–L*) Microscopic (*G–I*) and macroscopic (*J–L*) visualization of GUS activity in upper systemic leaves. (Bars = 200 μm.)

mal cells required at least 12 hr because only single infected cells were detected at this time p.i. Once cell-to-cell spread was initiated, however, movement occurred at a rate of approximately one cell every 2 hr. With this assay, the
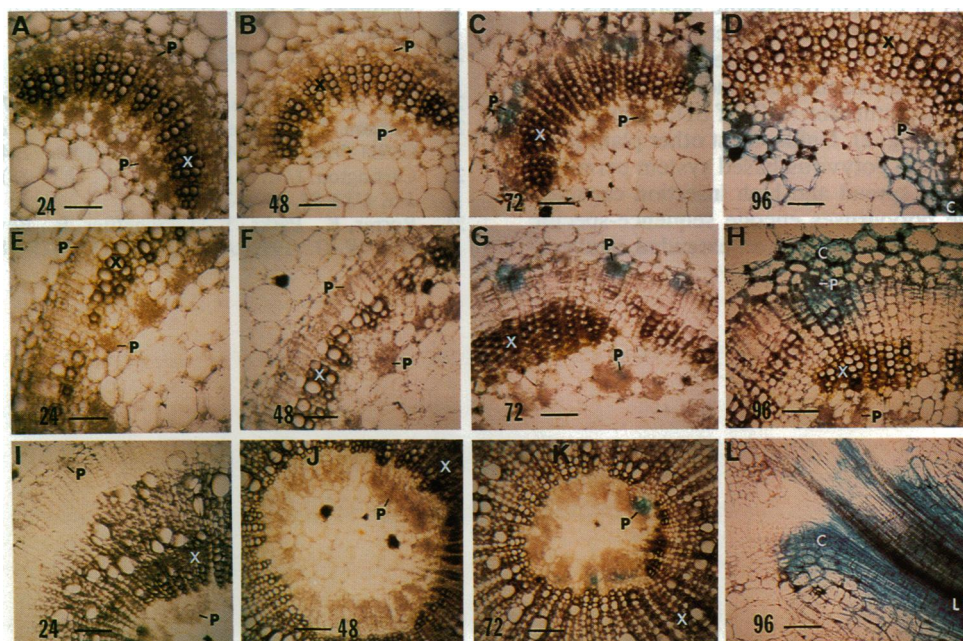

Fig. 6.   *In situ* localization of GUS activity in cross-sections of petioles, stems, and roots of plants infected by TEV–GUS. Sections were cut by hand at the times p.i. (hr) indicated at bottom of *A–L* and incubated with the histochemical substrate X-gluc. (*A–D*) Petioles. (*E–H*) Stems. (*I–L*) Roots. C, cortex; LR, lateral root; P, phloem; X, xylem. (Bars = 200 μm.)

TEV–GUS system will now permit the analysis of potyviral functions involved in virus movement in intact plants.

The timing of TEV–GUS replication after long-distance transport to upper (leaves and petioles) and lower (roots) tissues was similar (60–72 hr p.i.). The initial GUS-positive cells in systemic tissues were phloem-associated, suggesting that virus replication occurs first in cells connected to sieve elements. Although studies with other viruses have shed light on the viral proteins required for cell-to-cell movement in epidermal and mesophyll cells, little is known regarding the mechanisms of ingress into and egress from the plant vascular system (20, 21). The TEV–GUS model should allow investigations into the factors necessary for these phases of virus transport, as well as the rates of movement to and through various cell types and target tissues (such as roots—see Fig. 6L).

The ability to visualize virus-infected cells in whole plants may have wide application to investigations of virus–host interactions. Considering that the inability of plant viruses to infect certain hosts is the result of inhibition of cell-to-cell and/or long-distance movement (21), the nature of virus restriction in nonhosts and in hosts carrying resistance genes can be addressed easily. In virus–host combinations involving seed transmission, the identities of cell types supporting virus replication in reproductive or embryonic tissues can be analyzed. Likewise, application of this strategy should reveal the pathways of virus entry and spread after vector-mediated transmission. Tagged viruses such as TEV–GUS also represent ideal subjects to study evolution of genome sequences under various degrees of selection pressure. The frequencies of point mutation in essential (e.g., RNA polymerase), accessory (helper component), and superfluous (GUS) coding regions can be analyzed directly within a single genome. Additionally, the stepwise removal of nonessential sequences, as demonstrated in Fig. 4, will provide an important resource to study the factors that affect genome rearrangement and stabilization.

The TEV–GUS system demonstrates that potyviruses may have utility as replicating vectors for the introduction and expression of foreign genes in plants. A replicating vector capable of transporting foreign genes systemically through plants would circumvent the plant transformation and regeneration requirements of current transgenic approaches (22). The theoretical yield of protein products encoded by a potyvirus vector is extremely high because all virus genome-encoded proteins are synthesized in equimolar amounts. For TEV, capsid protein accounts for ≈1% of SDS-soluble protein in infected leaves (Fig. 2). Unlike most other plant RNA virus vectors (11–13), the potyvirus-based system permitted both efficient systemic spread and high insertion capacity. Finally, because the potyviruses encode sequence-specific proteinases, one of which recognizes an extended cleavage site motif that can be inserted into or around foreign proteins (23, 24), the potential for controlled proteolytic modification of engineered proteins is high.

1. Dougherty, W. G. & Carrington, J. C. (1988) *Annu. Rev. Phytopathol.* **26,** 123–143.
2. Riechmann, J. L., Lain, S. & Garcia, J. A. (1992) *J. Gen. Virol.* **73,** 1–16.
3. Carrington, J. C. & Dougherty, W. G. (1989) *J. Virol.* **61,** 2540–2548.
4. Carrington, J. C., Cary, S. M., Parks, T. D. & Dougherty, W. G. (1989) *EMBO J.* **8,** 365–370.
5. Verchot, J., Herndon, K. L. & Carrington, J. C. (1992) *Virology* **190,** 298–306.
6. Thornbury, D. W., Patterson, C. A., Dessens, J. T. & Pirone, T. P. (1990) *Virology* **178,** 1573–1578.
7. Bujarski, J. J., Ahlquist, P., Hall, T. C., Dreher, T. W. & Kaesberg, P. (1986) *EMBO J.* **5,** 1769–1774.
8. Pogue, G. P. & Hall, T. C. (1992) *J. Virol.* **66,** 674–684.
9. Meshi, T., Watanabe, Y., Saito, T., Sugimoto, A., Maeda, T. & Okada, Y. (1987) *EMBO J.* **6,** 2557–2563.
10. Petty, I. T. D., French, R., Jones, R. W. & Jackson, A. O. (1990) *EMBO J.* **9,** 3453–3457.
11. French, R., Janda, M. & Ahlquist, P. (1988) *Science* **231,** 1294–1297.
12. Takamatsu, N., Ishikawa, M., Meshi, T. & Okada, Y. (1987) *EMBO J.* **6,** 307–311.
13. Joshi, R. L., Joshi, V. & Ow, D. W. (1990) *EMBO J.* **9,** 2663–2669.
14. Carrington, J. C., Freed, D. D. & Oh, C.-S. (1990) *EMBO J.* **9,** 1347–1353.
15. Kunkel, T. A., Roberts, J. D. & Zakour, R. A. (1987) *Methods Enzymol.* **154,** 367–382.
16. Carrington, J. C. & Freed, D. D. (1990) *J. Virol.* **64,** 1590–1597.
17. Restrepo, M. A., Freed, D. D. & Carrington, J. C. (1990) *Plant Cell* **2,** 987–998.
18. Mavankal, G. & Rhoads, R. E. (1991) *Virology* **185,** 721–731.
19. Matthews, R. E. F. (1991) *Plant Virology* (Academic, New York).
20. Deom, C. M., Lapidot, M. & Beachy, R. N. (1992) *Cell* **69,** 221–224.
21. Hull, R. (1989) *Annu. Rev. Phytopathol.* **27,** 213–240.
22. Donson, J., Kearney, C. M., Hilf, M. E. & Dawson, W. O. (1991) *Proc. Natl. Acad. Sci. USA* **88,** 7204–7208.
23. Carrington, J. C. & Dougherty, W. G. (1988) *Proc. Natl. Acad. Sci. USA* **85,** 3391–3395.
24. Rorrer, K., Parks, T. D., Scheffler, B., Bevan, M. & Dougherty, W. G. (1992) *J. Gen. Virol.* **73,** 775–783.